Synthesis, Structural Characterisation, and Monte Carlo Simulation of the Magnetic Properties of the 3D-Stacked Honeycomb $Cs_n[\{Mn(N_3)_3\}_n]$ and the Irregular Double Chain $[\{N(C_2H_5)_4\}_n][\{Mn_2(N_3)_5(H_2O)\}_n]$

Mohamed A. S. Goher,[b] Joan Cano,[c] Yves Journaux,[c] Morsy A. M. Abu-Youssef,[d] Franz A. Mautner,[e] Albert Escuer,*[a] and Ramon Vicente[a]

Abstract: Two new polymeric manganese-azido systems with formula $Cs_n[\{Mn(N_3)_3\}_n]$ (**1**) and $[\{N(C_2H_5)_4\}_n][\{Mn_2(N_3)_5(H_2O)\}_n]$ (**2**) were synthesised and structurally characterised. Compound **1** crystallises in the $P2_1/n$ group and consists of a three-dimensional system with end-to-end and end-on azido bridges with the caesium atoms in the holes of the net. Magnetically, compound **1** is a rare case of a three-dimensional network with alternate ferro–antiferromagnetic interactions. Compound **2** crystallises in the $P\bar{1}$ group and consists of double chains of manganese atoms bridged by end-on and, the exceptional, (μ-1,1,1)-azido bridges. Magnetically, compound **2** shows net ferromagnetic behaviour. Exact fit of the magnetic data was performed for the two compounds by means of Monte Carlo simulations based on the Metropolis algorithm on sets of $10 \times 10 \times 10$ (**1**) and $1 \times 1 \times 320$ (**2**) $S = 5/2$ classical spin centres.

Keywords: azido bridges · magnetic properties · manganese · Monte Carlo simulations · N ligands

Introduction

Currently, more and more work in the field of magnetochemistry is devoted to the study of the magnetic properties of high-dimensional systems; this forces magnetochemists to develop new equations or methods to fit the susceptibility data, to search for uncommon EPR features or to permit the characterisation of cooperative phenomena such as molecular magnet behaviour. In recent years, the manganese(II)-azido derivatives have provided an exceptional number of unprecedented structural and magnetic properties. The main factor that permits such different kinds of properties is the extreme versatility of the azido ligand, which may act as an end-on (μ-1,1 or EO) or end-to-end (μ-1,3 or EE) bridge to give usually a ferromagnetic (FM) or antiferromagnetic (AF) coupling, respectively.[1] For extended systems such as one-dimensional chains, all kinds of interactions have been found: ferromagnetic EO chains,[2] antiferromagnetic EE chains[2, 3] or alternating FM–AF systems[2, 4] due to alternating EE/EO bridges. For two-dimensional systems, quadratic layers with EE bridges with AF coupling[5] and also alternating EE/EO systems[6], which magnetically shows alternating FM/AF coupling, have been characterised. Regular AF three-dimensional compounds have also been described with only EE azido bridges.[7] Some authors have introduced a second kind of bridging ligand such as 4,4′-bipyridine or bipirymidine, to obtain complicated two-dimensional or three-dimensional topologies.[8]

From our research in this field, we have characterised two new Mn-azido systems with caesium or tetraethylammonium countercations. The size of the cation determines a drastic variation in the structural arrangement: whereas $Cs_n[\{Mn(N_3)_3\}_n]$ (**1**) is a three-dimensional system that hosts the caesium atoms in the holes of the structure, $[\{N(C_2H_5)_4\}_n][\{Mn_2(N_3)_5(H_2O)\}_n]$ (**2**) consists of double chains of manganese atoms isolated by the large tetraethylammonium cations. The coordination modes of the azido bridges are exceptional for different reasons in each compound: in **1** layers of alternating EO/EE bridges are linked to each other by means of new EE bridges to give an FM/AF/AF three-dimensional system, whereas in **2** the manganese-azido chains (μ-1,1

[a] Dr. A. Escuer, Dr. R. Vicente
Departament de Química Inorgànica
Universitat de Barcelona, 08028 Barcelona (Spain)
Fax: (+34) 93-4907725
E-mail: aescuer@kripto.qui.ub.es

[b] Dr. M. A. S. Goher
Chemistry Department, Faculty of Science
Kuwait University, P.O. Box 5969 Safat, 13060 (Kuwait)

[c] Dr. J. Cano, Dr. Y. Journaux
Laboratoire de Chimie Inorganique, UMR 8613, CNRS
Université de Paris-Sud, 91405 Orsay (France)

[d] Dr. M. A. M. Abu-Youssef
Chemistry Department, Faculty of Science
Alexandria University (Egypt)

[e] Dr. F. A. Mautner
Institut für Physikalische und Theoretische Chemie
Technische Universität, 8010 Graz (Austria)

© WILEY-VCH Verlag GmbH, D-69451 Weinheim, 2000
0947-6539/00/0605-0778 $ 17.50+.50/0

bridges) are linked by the very rare (μ-1,1,1)-azido-bridging mode to give a ferromagnetic double-chain system.

Owing to the mathematical difficulties, it is impossible to derive the thermodynamic properties (magnetic susceptibility, specific heats, etc) of an extended network with so intricate topology of interactions. Till now, for Heisenberg extended networks, nobody has been able to go beyond the one-dimensional $S = 1/2$ model for the calculation of the exact partition function.[9] In the case of $S = 5/2$ systems, it is well established that spin may be treated as a classical vector. Even with this drastic approximation only simple systems, such as regular[10] and alternating[4b] chains, have been studied; only recently, more elaborated networks like the alternating honeycomb topology have been considered.[11] However, with this method of calculation it seems impossible to deal with systems like three-dimensional arrays or chains with complicated topology such as those presented in this paper. For these cases, Monte Carlo simulation seems to be the only possible method for deriving the thermodynamic properties. Therefore, with the aid of structural data, we present the analysis of the magnetic properties of $S = 5/2$ AF/AF/FM-stacked honeycomb three-dimensional lattices and FM/FM-alternating double chains using Monte Carlo simulation based on the Metropolis algorithm.[12]

Abstract in Catalan: *Han estat sintetitzats i caracteritzats estructuralment dos nous sistemes polimèrics manganès-azidur de fórmula $Cs_n[\{Mn(N_3)_3\}_n]$ (**1**) i $[\{N(C_2H_5)_4\}_n][\{Mn_2(N_3)_5(H_2O)\}_n]$ (**2**). El compost **1** cristallitza en el grup $P2_1/n$, essent un sistema tridimensional que presenta ponts azidur end-to-end i end-on, on els àtoms de cesi hi ocupen els buits de la xarxa. Magnèticament, el compost **1** és un dels rars exemples de xarxa 3-D amb alternància d'interaccions ferro- antiferromagnètiques. El compost **2** cristallitza en el grup $P\bar{1}$ i consisteix en cadenes dobles d'àtoms de manganès units per l'excepcional pont azidur μ-1,1,1. Magnèticament, aquest compost presenta un comportament global ferromagnètic. L'ajust exacte de les dades de susceptibilitat magnètica per tots dos compostos es va dur a terme mitjançant simulacions Monte Carlo basades en l'algoritme de Metropolis, utilitzant blocs de $10 \times 10 \times 10$ (**1**) i $1 \times 1 \times 320$ (**2**) espins clàssics $S = 5/2$.*

Results and Discussion

Description of the structure of $Cs_n[\{Mn(N_3)_3\}_n]$ (1): The structure consists of a three-dimensional manganese-azido network and isolated caesium cations. A labelled ORTEP plot of the asymmetric unit is shown in Figure 1. The three-dimensional system may be envisaged as parallel manganese-azido layers linked by means of *trans* end-to-end azido bridges, Figure 2 (right). The parallel layers contain pairs of manganese atoms bridged by two end-on azido bridges, which are linked to the four similar neighbouring units by means of four single end-to-end azido bridges, Figure 2 (left) . The topology of these layers is the same as that reported for the two-dimensional compounds $[\{Mn(L)_2(N_3)_2\}_n]$ with L = ethylisonicotinate, 3-acetylpyridine, 4-cyanopyridine or ethylnicotinate,[6] in which the apical positions are occupied by the pyridinic ligands. The MnN_6 environment is strongly asymmetric: equatorial bond lengths Mn1–N11 2.271(7) Å and axial Mn1–N31 and Mn1–N33B, 2.195(6) and 2.203(7), respectively. The bond angle Mn1–N11–Mn1A is 99.2(3)°, slightly lower than the typical bond angles of a doubly end-on azido unit. The Mn ··· Mn distance in this unit is 3.424(2) Å. The end-to-end azido bridges between these dimeric units have Mn1-N21-N22 and Mn1-N23C-N22C bond angles of 128.7(6)° and 122.2(6)°, respectively, whereas the axial Mn1-N31-N32 and Mn1-N33B-N32B bond angles have the larger values of 149.7(6)° and 152.5(7)°, respectively. Torsion angles Mn1-N21-N23-Mn1B and Mn1-N31-N33-Mn1C are 159.2(4)° and 175.2(7)°, respectively. According to the bond and torsion angles, the Mn ··· Mn distances through the EE azido bridges are 6.127(3) Å and 6.522(3) Å.

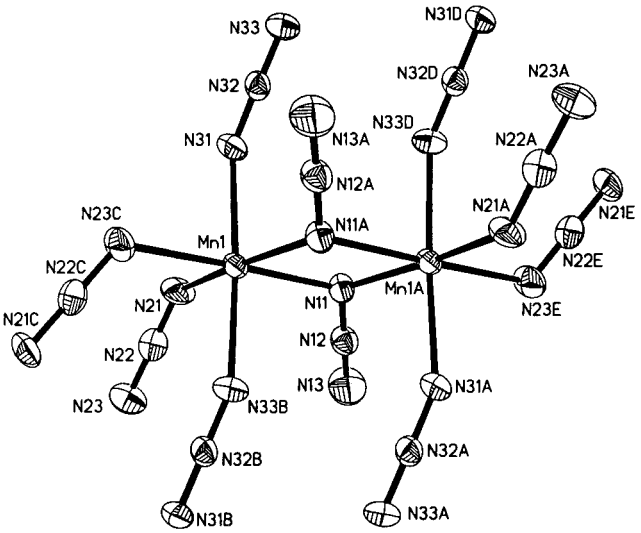

Figure 1. Ortep drawing for $Cs_n[\{Mn(N_3)_3\}_n]$ (**1**). Ellipsoids at 50% probability level.

Description of the structure of $[\{N(C_2H_5)_4\}_n][\{Mn_2(N_3)_5(H_2O)\}_n]$ (2): The structure consists of polymeric $[\{Mn_2(N_3)_5(H_2O)\}_n]^-$ chains oriented along the *a* axis of the unit cell, well isolated by $[N(C_2H_5)_4]^+$ counter ions. A labelled ORTEP plot of the asymmetric unit is shown in Figure 3. Both manganese atoms have distorted octahedral environments. The octahedron of Mn1 is formed by nitrogen atoms of six azido groups, whereas Mn2 is surrounded by five azido ligands and one water molecule. Each octahedron has common N–N edges with four neighbouring octahedra, thus forming double chains of polyhedra, Figure 4. All azido groups are only bonded with one nitrogen atom to the manganese(II) centre(s) and so act in the EO fashion. As a consequence of the double chain with common edge-sharing polyhedra, three types of azido ligands occur: one single-coordinate azido group (N51), two (μ-1,1)-azido bridges (N11 and N41) and two (μ-1,1,1)-azido bridges (N21 and N31). This is a very rare case, in which three different types of azido ligands are observed in the same coordination compound.

The changes of the electronic properties of the manganese(II)-azido bond and of bonds within the azido ligand itself,

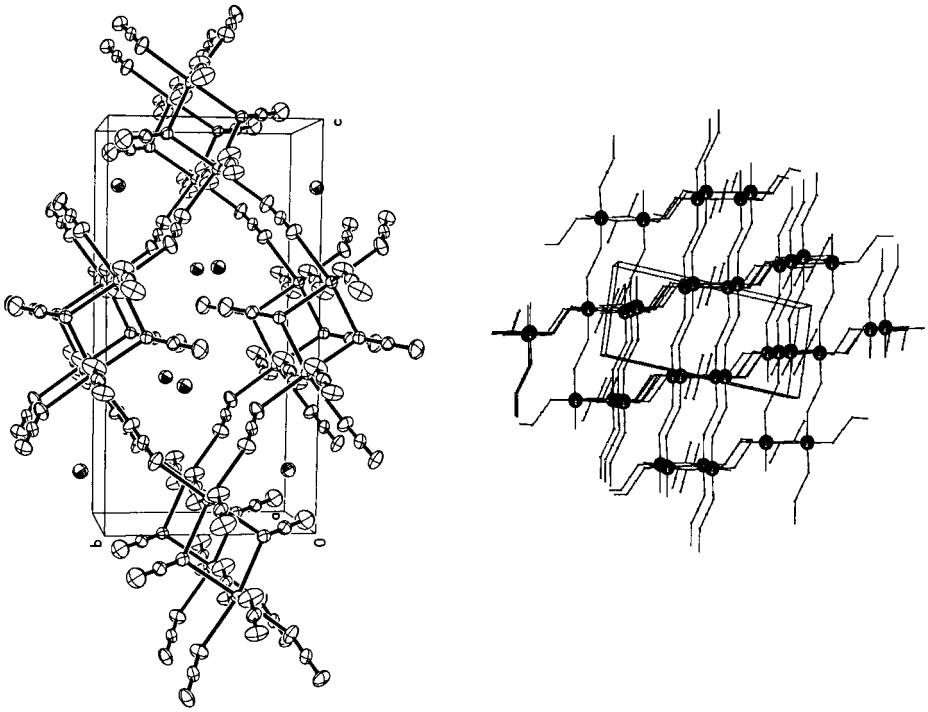

Figure 2. View of the EE-azido bridge arrangement between the layers (right) and the alternating EE /EO bridges inside the planes (left) for $Cs_n[\{Mn(N_3)_3\}_n]$ (**1**).

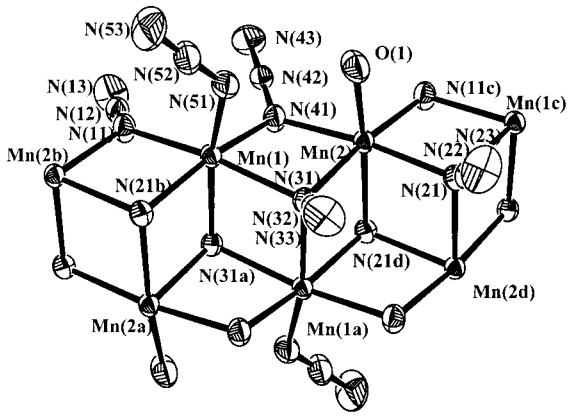

Figure 3. Ortep plot for $[\{N(C_2H_5)_4\}_n][\{Mn_2(N_3)_5(H_2O)\}_n]$ (**2**). Ellipsoids at 50% probability level.

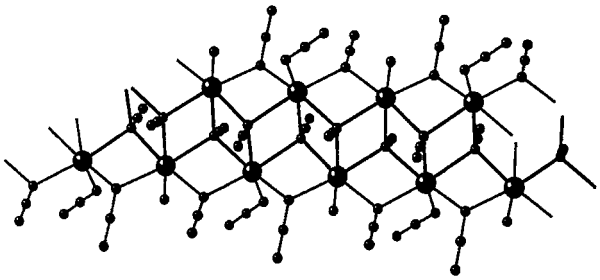

Figure 4. View of the double chain arrangement for $[\{N(C_2H_5)_4\}_n]$-$[\{Mn_2(N_3)_5(H_2O)\}_n]$ (**2**).

with respect to the three different coordination modes of the azido groups, is accompanied by variations in the observed geometrical parameters. The Mn–N (azido) bond lengths are well separated for each type of azido ligand and increase from single-coordinate (a) [2.153(3) Å] to (μ-1,1)-bridging (b) [2.187(3) to 2.221(3) Å] to (μ-1,1,1)-bridging azido groups (c) [2.284(3) to 2.330(3) Å]. In addition the Δd values (Δd: difference between N–N bond distances within an azido group) increase from 0.01 Å for ligand type a, to 0.06 Å for type b and up to 0.10 Å for type c. The Mn–N–N bond angles decrease from ligand type a [129.2(3)°] to type b [128.4(3) to 122.7(3), mean: 126.1°] to type c [113.8(2) to 123.9(2), mean: 119.1°], whereas the N–N–N bond angles remain constant within experimental error [mean 178.8(5)°]. All the Mn···Mn distances are very close to 3.5 Å.

The dependence of the structure of the manganese/azido $C^+[Mn(N_3)_3]^-$ system on the countercation should be noted: the caesium compound has a close three-dimensional structure, with short Mn···Mn distances derived from the EO azido bridges, whereas for the larger cation tetramethylammonium, the compound shows only EE bridges in a more open three-dimensional network, in which the cation is placed inside the cubic holes of a perovskite-like structure.[7b] For larger cations, such as tetraethylammonium or tetraphenylphosphonium[13] three-dimensional structures become inadequate to host the cation and so dimensionality is lost; this results in one-dimensional arrays or discrete molecules, respectively. This effect gives a simple way to tune the dimensionality of this kind of system, and shows that small countercations may favour high-dimensional compounds.

The (μ-1,1,1)-azido bridge: To our knowledge, simultaneous coordination of three modes of the azido ligand in the same compound has been observed in the analogous polymeric Zn-complex[14] with NMe_4^+ as counterion; this complex has the same set of terminal, (μ-1,1)- and (μ-1,1,1)-azido ligands. Three different azido bridges (μ-1,3, μ-1,1 and also μ-1,1,1) were found in the polynuclear cobalt(II) complex with empirical formula $Cs_2[Co_3(N_3)_8]$.[15]

In addition to the typical (μ-1,1)- and (μ-1,3)-azido bridges between two metallic centres, several (μ-1,1,1)-azido bridges between three metallic centres have been found. The μ-1,1,1 coordination mode appears generally related with discrete triangular or cubane-like structures. In addition to the above-mentioned complexes $Cs_2[Co_3(N_3)_8]$ (triangular) and $[\{N(CH_3)_4\}_n][\{Zn_2(N_3)_5(H_2O)\}_n]$ (three-dimesional), the μ-1,1,1 bridging mode has been observed only seven times. In the 3:2 complex of azido-Cu^{II} with 2-benzoylpyridine, an asymmetric (μ-1,1,1)-azido bridge was reported, with two short Cu–N bonds and one semi-coordinative Cu–N bond.[16]

© WILEY-VCH Verlag GmbH, D-69451 Weinheim, 2000
0947-6539/00/0605-0780 $ 17.50+.50/0 *Chem. Eur. J.* **2000**, *6*, No. 5

(μ-1,1,1)-azido bridging was also reported for a triangular titanium compound[17]; the remaining (μ-1,1,1)-azido bridges were found in five crystal structures of cubane-like tetrameric clusters with platinum(II),[18] manganese(III)[19] and three examples with nickel(II)[20] as metal centres. Magnetic behaviour for this coordination mode was reported for the cubane nickel systems; these complexes have weak ferromagnetic superexchange interaction due to the low M-N-M bond angles.

Magnetic measurements and coupling constants calculation: Susceptibility measurements were performed between 300–4 K for both compounds. The temperature dependence of the molar magnetic susceptibility and the $\chi_M T$ product for **1** is depicted in Figure 5. $\chi_M T$ decreases continuously as the

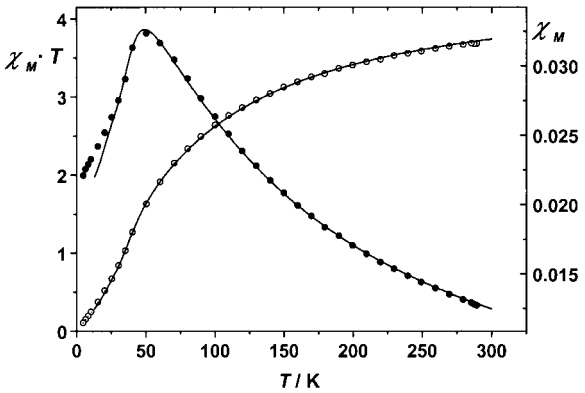

Figure 5. Plot of the molar susceptibility (filled circles) and $\chi_M T$ product versus T (open circles) for $Cs_n[\{Mn(N_3)_3\}_n]$ (**1**). Solid lines show the best fit of the data (see text).

temperature decreases, from 3.68 $cm^3 K mol^{-1}$ at room temperature, which is a slightly lower value than that expected for magnetically isolated Mn^{II} ions, towards to zero at low temperature. At 50 K the molar susceptibility has a maximum equal to 3.23×10^{-2} $cm^3 mol^{-1}$, which indicates a three-dimensional antiferromagnetic ordering. In contrast, $\chi_M T$ for compound **2** increases from the expected value for magnetically isolated Mn^{II} ions at room temperature to reach the maximum value of 22.8 $cm^3 K mol^{-1}$ at 6 K; this indicates an overall ferromagnetic response (Figure 6).

The different global behaviour for the two compounds may be envisaged from qualitative arguments: in **1**, the azido bridges have two modes of coordination, namely the μ-1,1 and μ-1,3 modes, whereas in **2** only EO bridges in the form of μ-1,1 and μ-1,1,1 modes are present. It is well established that the (μ-1,1)-azido bridge generally favours ferromagnetic coupling,[21] but it has been experimentally proved that this bridge can lead also to antiferromagnetic coupling between copper(II) centres for large bridging M–N(azido)–M angles.[22] Recently, the magnetic response of the EO azido bridges as a function of the M–N–M bond angle has been studied by means of DFT calculations,[23] showing that for M = Mn, FM behaviour should be found for Mn–N–Mn bond angles larger than 98°. On this basis, moderate or weak FM coupling should be expected for all the EO bridges in the two compounds, including the μ-1,1,1 bridges. However, the (μ-1,3)-azido

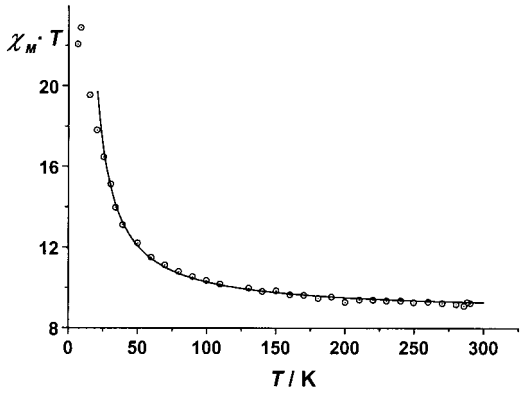

Figure 6. Plot of the $\chi_M T$ product versus T for $[\{N(C_2H_5)_4\}_n][\{Mn_2(N_3)_5(H_2O)\}_n]$ (**2**). Solid lines show the best fit of the data (see text).

bridge is known to mediate strong antiferromagnetic coupling between the magnetic ions. Recent MO calculations and experimental results show that for d^8 and d^9 cations such as copper(II) or nickel(II), FM coupling may be found for some extreme bond or torsion angles,[24] but for d^5 cations such as manganese(II) fairly strong coupling is expected in any case. The spin coupling topology for **1** indicates a ground state $S = 0$ and overall antiferromagnetic behaviour, whereas net weak ferromagnetic coupling is reasonably expected for **2**.

Quantitative analysis of the coupling constant parameters for **1** may be performed from the interaction topology shown in Figure 7; this leads to the Hamiltonian given in Equation (1). For **1**, one constant coupling was rigorously taken into account for each different bridge. The summation Σ goes over all the nearest-neighbour pairs on the lattices, S_n is the classical spin operator at the nth site and J_1, J_2 and J_3 are the

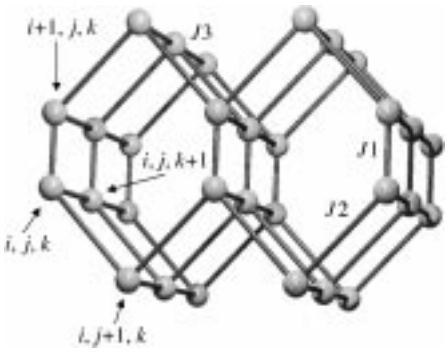

Figure 7. Interaction scheme for the three J constant coupling parameters used in the Hamiltonian [Eq. (1)]. In order to simplify the drawing, only the three-dimensional manganese skeleton of **1** is shown.

$$H = -J_1 \sum_{i+j(\mathrm{odd}),k} S_{i,j,k} S_{i+1,j,k} - J_2 \sum_{i,j,k} S_{i,j,k} S_{i,j+1,k} - J_3 \sum_{i,j,k} S_{i,j,k} S_{i,j,k+1} \quad (1)$$

exchange coupling constants. In the light of structural data and the above considerations, the three-dimensional spin topology consists of an antiferromagnetic chain (J_2) coupled ferromagnetically and antiferromagnetically with other chains along perpendicular directions to create a honeycomb (J_1, J_2) and a square (J_2, J_3) layer, respectively.

The topology of interaction in compound **2** is proposed in Figure 8; this leads to the Hamiltonian given in Equation (2).

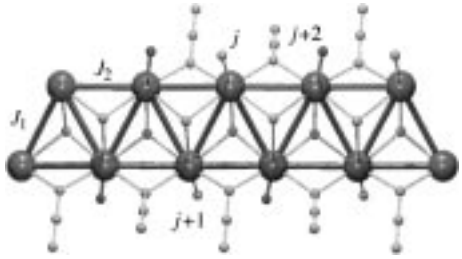

Figure 8. Double chain interaction scheme for the two J constant coupling parameters used in the Hamiltonian [Eq. (2)]. To simplify the calculations, one J parameter for the μ-1,1 bridges along the chains and one J parameter for the crossing μ-1,1,1 bridges were assumed.

In this case, one J_1 parameter between the two chains and one J_2 constant coupling along each individual chain were assumed, in accordance with the similar bonding parameters. Positive signs for both J parameters should be expected.

$$H = -J_1 \sum_j S_j S_{j+1} - J_2 \sum_j S_j S_{j+2} \quad (2)$$

In order to make a quantitative comparison, the classic spin is scaled according to the factor $S_j = [S_j \cdot (S_j + 1)]^{1/2}$. The Metropolis algorithm[12] generates a sampling of states distributed according to the Boltzmann distribution. Equation (3) gives the relationship between the magnetic susceptibility, χ, and magnetic fluctuation, M. In Equation (3) $\langle M \rangle$ and $\langle M^2 \rangle$ are the average values of the magnetisation and the square of the magnetisation.

$$\chi = \frac{(\langle M^2 \rangle - \langle M \rangle^2)}{kT} \quad (3)$$

10^5 Monte Carlo steps (MCS) were performed per site and the first 10^4 were discarded as the initial transient stage. To avoid freezing the spin configuration, a low cooling rate was used according to the equation $T_{n+1} = 0.95 \times T_n$, in which T stands for temperature. Samples of $10 \times 10 \times 10$ and $1 \times 1 \times 320$ were used for **1** and **2**, respectively. These samples are large enough to prevent any finite size effects. To avoid perturbation from the edge of the sample and to speed up convergence toward the infinite lattice limit, periodic boundary conditions (PBC) were used.[25]

The Monte Carlo simulation confirms the previous analysis. A good fit of the experimental data in the 300–25 K temperature range is only obtained with $|J_2| > |J_3| > |J_1|$, as shown in Figure 5. Then the best agreement is obtained with the following parameters: $g = 2.029 \pm 0.021$, $J_1 = 0.76 \pm 0.21$ cm^{-1}, $J_2 = -4.3 \pm 0.3$ cm^{-1} and $J_3 = -3.3 \pm 0.6$ cm^{-1}. The agreement factor F defined as $F = \Sigma(\chi_M T_{exp} - \chi_M T_{theor})^2 / \Sigma(\chi_M T_{exp})^2$ is equal to 4.7×10^{-5} and R^2 is equal to 0.99991. We found that the Monte Carlo method, which considers a classic spin Hamiltonian, describes the dependence of magnetic susceptibility on temperature, even at low temperature, for the cubic three-dimensional network well.[26] However, there is a small discrepancy between the theoretical and experimental data at $T < 25$ K for **1**. This discrepancy is attributed to the quantum effects, which are more important at low temperature and cannot be described by a classic spin model. These quantum effects are more important in **1** because the interaction density per site is smaller than in a three-dimensional cubic network.

For **2**, good agreements between experimental and simulated data are obtained by using two different sets of parameters $g = 2.001 \pm 0.003$, $J_1 = 1.57 \pm 0.03$ cm^{-1} and $J_2 = 0.29 \pm 0.04$ cm^{-1} or $g = 2.007 \pm 0.005$, $J_1 = 0.66 \pm 0.04$ cm^{-1} and $J_2 = 1.07 \pm 0.03$ cm^{-1} and R equal to 9.7×10^{-5} and 8.8×10^{-5} (Figure 6). A careful examination of the structure (angles, bond lengths) does not reveal the set of parameters with the best physical meaning. Furthermore, the determination of ferromagnetic interactions is always fairly inaccurate[27] and the use of a simplified topology of interaction does not permit unambiguous assignation.

In both cases, the J values found for the interaction through the (μ-1,1)- or (μ-1,3)-azido bridge are similar to those found in more simple systems. There are few complexes in the literature of manganese(II) complexes with only a single EE-azido group as bridging ligand, but some reported compounds permit comparison with our results: J values of -1.4, -2.2 and -3.8 cm^{-1} were reported for $[\{Mn(L)_2(N_3)_2\}_n]$ systems (L = pyridine,[6c] methylisonicotinate[5b] and 4-acetylpyridine[6c]), or -1.2 cm^{-1} for the three-dimensional $(NMe_4)[Mn(N_3)_3]$ compound.[7b] We have obtained similar values for **1** (-4.3 and -3.3 cm^{-1}) that nicely confirm the predicted dependence of the antiferromagnetic component of J on the magnitude of bond angles in the bridging region.[6c] However, for the systems with a double (μ-1,1)-azido bridge, we obtained a J value close to 1 cm^{-1}; this is associated with Mn–N–Mn bond angles lower than 100° (99.2° for **1** and a mean value of 99.4° for **2**). Only two complexes with EO bridges only have been reported in the literature, the $[\{Mn(2\text{-bzpy})(N_3)_2\}_n]$ chain system[2] with Mn–N–Mn bond angles around 100° and $J = 0.8$ cm^{-1}, and the dinuclear compound $[\{Mn(terpy)\{(\mu\text{-}1,1)\text{-}N_3\}(N_3)\}_2]$ with an Mn–N–Mn bond angle of 104.6° and greater coupling, $J = 2.4$ cm^{-1}.[28] Lower J values for bond angles close to or lower than 100° and clearly greater coupling at 104.6° corroborate closely with the DFT calculations performed by Ruiz et al.,[23] who proposed the crossover from ferro- to antiferromagnetism at 98°.

Experimental Section

Synthesis: Warning! The reported azido complexes are potentially explosive. Only a small amount of material should be prepared, and it should be handled with care.

$Cs_n[\{Mn(N_3)_3\}_n]$ (1): $Mn(NO_3)_2 \cdot 4H_2O$ (3.2 g, 12.7 mmol) was mixed with cold saturated aqueous solution of CsN_3 (13.5 M, 15 mL). Saturated HN_3 in distilled water (15 mL) was added dropwise until a crude precipitate was formed. MeOH (20 mL) was added, and the mixture was placed over a 95 °C water bath for 1 hour. The hot turbid solution was filtered. Within 5 days transparent green crystals were formed by stepwise cooling of the final clear solution from 95 °C to 35 °C. Yield 30 %; $CsMnN_9$ (313.90): calcd Cs 42.34, Mn 17.50, N 40.16; found Cs 42.25, Mn 17.38, N 40.37.

$[\{N(C_2H_5)_4\}_n][\{Mn_2(N_3)_5(H_2O)\}_n]$ (2): Solid $Mn(NO_3)_2 \cdot 4H_2O$ (1.2 g, 4.8 mmol) followed by aqueous saturated HN_3 (15 mL) and MeOH (25 mL) were added to an aqueous solution of $N(C_2H_5)_4(N_3)$ (40 %, 10 mL). The mixture was placed on a 95 °C water bath for 1 hour and was filtered. The filtrate was then placed in a 50 °C water bath overnight. The solution was filtered once again and left for several days to give colourless needles of **2** suitable for X-ray measurements. Yield 55 %; $Mn_2C_8H_{22}N_{16}O$ (468.24): calcd C 20.52, H 4.74, N 47.86, Mn 23.46; found C 20.60, H 4.85, N 47.70, Mn 23.50.

IR spectra: The IR spectra of $Cs_n[\{Mn(N_3)_3\}_n]$ (**1**) shows asymmetric azido-group vibrations ($\tilde{\nu}_{as}$ N_3) centred around 2115, 2075 and 2062 cm^{-1} (vs.), and

© WILEY-VCH Verlag GmbH, D-69451 Weinheim, 2000
0947-6539/00/0605-0782 $ 17.50+.50/0 Chem. Eur. J. 2000, 6, No. 5

three bands centred at 1326 (s), 1286 (w) and 1226 (vw) cm^{-1} that correspond to the symmetric N_3 stretching. The strong band which appears at 1326 cm^{-1} should be assigned to the stretching of the EE-azido group, whereas the other two weak bands should correspond to the slightly asymmetric EE bridges. Bending of the azido ligands also appears as three bands at 652, 613 and 602 cm^{-1} with medium absorption.

The IR spectra of the complex $[\{N(C_2H_5)_4\}_n][\{Mn_2(N_3)_5(H_2O)\}_n]$ (**2**) show a broad moderate band attributed to the coordinated water at about 3370 cm^{-1} and a moderate band for the C–H vibrations of the $[N(C_2H_5)_4]^+$ counterion at 2991 cm^{-1}. In the 2000–2100 cm^{-1} region the complex shows very strong overlapping bands assigned to the asymmetric azido group vibrations (ν_{as} N_3) centred at 2044 (vs) and 2096 (vs) cm^{-1}. Medium to strong bands are observed at approximately 1300 cm^{-1}, which supports the asymmetric nature of the azido groups.

X-ray crystallography of $Cs_n[\{Mn(N_3)_3\}_n]$ (1) and $[\{N(C_2H_5)_4\}_n][\{Mn_2(N_3)_5(H_2O)\}_n]$ (2): The X-ray single-crystal data for both compounds were collected on a modified STOE four-circle diffractometer. Crystal size: $0.18 \times 0.15 \times 0.13$ mm for **1** and $0.45 \times 0.22 \times 0.22$ mm for **2**. The crystallographic data, the conditions for the intensity data collection and some features of the structure refinements are listed in Table 1. Graphite-monochromatized $Mo_{K\alpha}$ radiation ($\lambda = 0.71069$ Å) and the ω-scan technique were used to collect the data sets. The accurate unit-cell parameters were determined from automatic centring of 36 reflections ($9.7^\circ < \theta < 14.8^\circ$) for **1** and 28 reflections ($6.0^\circ < \theta < 11.0^\circ$) for **2** and were refined by least-squares methods. A total of 1285 reflections (1021 independent reflections, $R_{int} = 0.0406$) were collected for **1** in the range $3.48^\circ < \theta < 25.20^\circ$ and 4671 reflections (4150 independent reflections; $R_{int} = 0.0301$) for **2** in the range $2.88^\circ < \theta < 27.50^\circ$. Observed intensity decay of control reflections (0 2 3; −1 0 −5; 2 −1 1) was 7% for **1** and 16% for control reflections (2 2 0; −2 −1 3; −2 1 2) of **2**. Corrections were applied for Lorentz polarization effects, for intensity decay and for absorption by using the DIFABS[29] computer program (range of normalised transmission factors: 0.236–1.000 for **1** and 0.441–1.000 for **2**) . The structures were solved by Patterson methods by using the SHELXS-86[30] computer program, and refined by full-matrix least-squares methods on F for **1**, by using the SHELX-76 program[31], and on F^2 for **2**, by using the SHELXL-93[32] program incorporated in the SHELXTL/PC V 5.03[33] program library and the graphics program PLUTON[34]. All non-hydrogen atoms were refined anisotropically. The hydrogen atoms of **2** were obtained from ΔF maps, subsequently fixed geometrically and assigned with isotropic displacement factors (eight common ones for H atoms of each parent C atom of NEt_4 counterion). The final R indices were 0.0343 and 0.0559 for **1** and **2**, respectively, for all observed reflections. Number of refined parameters were 100 (**1**) and 264 (**2**). Maximum and minimum peaks in the final difference Fourier syntheses were 0.89 and −0.88 e $Å^{-3}$ (**1**), and 1.466 and −0.565 e $Å^{-3}$ in the vicinity of metal centres (**2**). Significant bond parameters for **1** and **2** are given in Tables 2 and 3, respectively.

Table 1. Crystal data and structure refinement for $Cs_n[\{Mn(N_3)_3\}_n]$ (**1**), and $[\{N(C_2H_5)_4\}_n][\{Mn_2(N_3)_5(H_2O)\}_n]$ (**2**).

	1	**2**
formula	$CsMnN_9$	$C_8H_{22}Mn_2N_{16}O$
M_w	319.91	468.30
space group	$P2_1/n$	$P\bar{1}$
a [Å]	6.5520(10)	6.873(3)
b [Å]	7.557(2)	11.600(5)
c [Å]	14.947(5)	13.000(5)
α [°]	90.0	70.54(3)
β [°]	93.47(2)	84.84(3)
γ [°]	90.0	88.89(3)
V [Å^3]	735.3(3)	973.2(7)
Z	4	2
T [°C]	22(2)	20(2)
ρ_{calcd} [g cm^{-3}]	2.836	1.598
$\mu(Mo_{K\alpha})$ [mm^{-1}]	6.62	1.334
R[a]	0.0343	0.0559
wR[b] or wR^2[c]	0.0354[b]	0.1430[c]

[a] $R(F_o) = \Sigma F_o - F_c / \Sigma F_o$. [b] $wR = [\Sigma w(F_o - k F_c)^2 / \Sigma F_o^2]^{1/2}$. [c] $wR(F_o)^2 = \{\Sigma[w((F_o)^2 - (F_c)^2)^2] / \Sigma[w((F_o)^2)^2]\}^{1/2}$.

Further details on the crystal structure investigation of **1** may be obtained from the Fachinformationszentrum Karlsruhe, D-76344 Eggenstein-Leopoldshafen, Germany (fax: (+49) 7247-808-666; E-mail: crysdata@fiz-karlsruhe.de), on quoting the depository number CSD-410810.

Crystallographic data (excluding structure factors) for the structure **2** reported in this paper have been deposited with the Cambridge Crystallographic Data Centre as supplementary publication no. CCDC-120665. Copies of the data can be obtained free of charge on application to CCDC, 12 Union Road, Cambridge CB2 1EZ, UK (fax: (+44) 1223-336-033; E-mail: deposit@ccdc.cam.ac.uk).

Table 2. Selected bond lengths [Å] and angles [°] for $Cs_n[\{Mn(N_3)_3\}_n]$ (**1**).

manganese environment			
Mn1-N11	2.271(7)	Mn1–N11a	2.223(6)
Mn1–N21	2.252(8)	Mn1–N23c	2.233(8)
Mn1–N31	2.195(6)	Mn1–N33b	2.203(7)
Mn1 ··· Mn	6.127(3)	Mn1 ··· Mn	6.522(3)
Mn1 ··· Mn	3.424(3)		
azido bridges			
N11–N12	1.190(9)	N12–N13	1.130(11)
N21–N22	1.169(9)	N22–N23	1.200(9)
N31–N32	1.171(8)	N32–N33	1.147(9)
Mn1 ·· Cs1	4.154(2)	Mn1 ·· Cs1g	4.681(2)
Mn1 ·· Cs1h	4.132(2)	Cs1 ·· Cs1h	4.881(2)
Cs1 ·· N11	3.242(6)	Cs1 ·· N13a	3.195(9)
Cs1 ·· N21	3.507(7)	Cs1 ·· N23a	3.439(7)
Cs1 ·· N31	3.433(9)	Cs1 ·· N13p	3.261(9)
Cs1 ·· N21m	3.295(7)	Cs1 ·· N31m	3.236(8)
Cs1 ·· N23e	3.341(7)		
manganese environment			
N11-Mn1-N11a	80.8(2)	Mn1-N11-N12	119.2(5)
N11-Mn1-N21	88.2(3)	Mn1a-N11-N12	122.9(5)
N11-Mn1-N23c	177.9(2)	Mn1-N11-Mn1a	99.2(3)
N11-Mn1-N31	93.8(3)	Mn1-N21-N22	128.7(6)
N11-Mn1-N33b	89.4(3)	Mn1-N23c-N22c	122.2(6)
N11a-Mn1-N21	168.6(3)	Mn1-N31-N32	149.7(6)
N11a-Mn1-N23c	101.2(3)	Mn1-N33b-N32b	52.5(7)
N11a-Mn1-N31	91.2(3)		
N11a-Mn1-N33b	90.9(3)		
azido bridges			
N21-Mn1-N23c	89.9(3)	N11-N12-N13	177.3(8)
N21-Mn1-N31	87.0(3)	N21-N22-N23	179.4(8)
N21-Mn1-N33b	91.5(3)	N31-N32-N33	179.1(9)
N23c-Mn1-N31	87.0(3)		
N23c-Mn1-N33b	89.7(3)		
N31-Mn1-N33b	176.4(3)		

Acknowledgements

This research was partially supported by CICYT (Grant PB96/0163) and OENB (grant 6630). F.A.M and M.A.M.A.-Y thank Prof. C. Kratky and Dr. Belaj (University of Graz) for use of experimental equipment. J.C. is indebted to the European Commission for a Marie Curie grant from the Training and Mobility program (contract No. ERBFMBICT972211).

[1] J. Ribas, A. Escuer, M. Monfort, R. Vicente, R. Cortés, L. Lezama, T. Rojo, *Coord. Chem. Rev.* **1999**, *193–195*, 1027.
[2] M. A. M. Abu-Youssef, A. Escuer, D. Gatteschi, M. A. S. Goher, F. A. Mautner, R. Vicente, *Inorg. Chem.* **1999**, *38*, 5716.
[3] A. Escuer, R. Vicente, M. A. S. Goher, F. A. Mautner, *Inorg. Chem.* **1998**, *37*, 782.

Table 3. Selected bond lengths [Å] and angles [°] for $[\{N(C_2H_5)_4\}_n]$-$[\{Mn_2(N_3)_5(H_2O)\}_n]$ (**2**).

manganese environment			
Mn1–N11	2.218(3)	Mn2–O1	2.187(3)
Mn1–N21b	2.314(3)	Mn2–N11c	2.187(3)
Mn1–N31	2.330(3)	Mn2–N21	2.286(3)
Mn1–N31a	2.284(3)	Mn2–N21d	2.304(3)
Mn1–N41	2.221(3)	Mn2–N31	2.301(3)
Mn1–N51	2.153(3)	Mn2–N41	2.201(3)
Mn1 ··· Mn1a	3.553(2)	Mn1 ··· Mn2b	3.447(2)
Mn1 ··· Mn2	3.432(2)	Mn1 ··· Mn2d	3.472(2)
Mn1 ··· Mn2a	3.505(2)		
azido ligands			
N11–N12	1.201(5)	N12–N13	1.135(5)
N21–N22	1.226(4)	N22–N23	1.127(5)
N31–N32	1.216(4)	N32–N33	1.118(5)
N41–N42	1.204(4)	N42–N43	1.141(5)
N51–N52	1.177(5)	N52–N53	1.167(5)
manganese environment			
N11-Mn1-N21b	79.3(1)	O1-Mn2-N11c	97.6(1)
N11-Mn1-N31	171.2(1)	O1-Mn2-N21	94.2(1)
N11-Mn1-N31a	91.8(1)	O1-Mn2-N21d	165.0(1)
N11-Mn1-N41	100.3(1)	O1-Mn2-N31	85.3(1)
N11-Mn1-N51	102.8(1)	O1-Mn2-N41	89.3(1)
N21b-Mn1-N31	99.0(1)	N11c-Mn2-N21	80.5(1)
N21b-Mn1-N31a	80.7(1)	N11c-Mn2-N21d	95.9(1)
N21b-Mn1-N41	169.6(1)	N11c-Mn2-N31	173.7(1)
N21b-Mn1-N51	93.2(1)	N11c-Mn2-N41	104.7(1)
N31-Mn1-N31a	79.3(1)	N21-Mn2-N21d	81.7(1)
N31-Mn1-N41	79.8(1)	N21-Mn2-N31	93.7(1)
N31-Mn1-N51	85.9(1)	N21-Mn2-N41	173.3(1)
N31a-Mn1-N41	88.9(1)	N21d-Mn2-N31	80.6(1)
N31a-Mn1-N51	162.9(1)	N21d-Mn2-N41	93.4(1)
N41-Mn1-N51	97.0(1)	N31-Mn2-N41	80.8(1)
Mn1-N11) N12	128.3(3)	Mn2-N21-N22	119.3(2)
Mn1-N31-N32	118.9(2)	Mn2-N31-N32	123.9(2)
Mn1-N41-N42	122.7(3)	Mn2-N41-N42	128.4(2)
Mn1-N51-N52	129.2(3)	Mn2b-N11-N12	124.9(3)
Mn1a-N31-N32	113.8(2)	Mn2d-N21-N22	122.2(3)
Mn1c-N21-N22	116.4(2)	Mn1-N31-Mn1a	100.7(1)
Mn1-N31-Mn2	95.6(1)	Mn1-N41-Mn2	101.8(1)
Mn1-N11-Mn2b	103.0(1)	Mn1a-N31-Mn2	99.7(1)
Mn1c-N21-Mn2	97.1(1)	Mn1c-N21-Mn2d	98.8(1)
Mn2-N21-Mn2d	98.3(1)		
azido bridges			
N11-N12-N13	179.3(5)	N41-N42-N43	179.0(4)
N21-N22-N23	178.5(5)	N51-N52-N53	178.4(5)
N31-N32-N33	179.1(4)		

[4] a) M. A. M. Abu-Youssef, A. Escuer, M. A. S. Goher, F. A. Mautner, R. Vicente, *Eur. J. Inorg. Chem.* **1999**, 687; b) R. Cortés, M. Drillon, X. Solans, L. Lezama, T. Rojo, *Inorg. Chem.* **1997**, *36*, 677.

[5] a) A. Escuer, R. Vicente, M. A. S. Goher, F. A. Mautner, *Inorg. Chem.* **1995**, *34*, 5707; b) A. Escuer, R. Vicente, M. A. S. Goher, F. A. Mautner, *J. Chem. Soc. Dalton Trans.* **1997**, 4431.

[6] a) M. A. S. Goher, N. A. Al-Salem, F. A. Mautner, *J. Coord. Chem.* **1998**, *44*, 119; b) A. Escuer, R. Vicente, F. A. Mautner, M. A. S. Goher, *Inorg. Chem.* **1997**, *36*, 3440; c) A. Escuer, R. Vicente, M. A. S. Goher, F. A. Mautner, *Inorg. Chem.* **1996**, *35*, 6386.

[7] a) M. A. S. Goher, F. A. Mautner, *Croat. Chem. Acta* **1990**, *63*, 559; b) F. A. Mautner, R. Cortés, L. Lezama, T. Rojo, *Angew. Chem.* **1996**, *108*, 96; *Angew. Chem. Int. Ed. Engl.* **1996**, *35*, 78.

[8] a) H. Y. Shen, D. Z. Liao, Z. H. Jiang, S. P. Yan, B. W. Sun, G. L. Wang, X. K. Yao, H. G. Wang, *Chem. Lett.* **1998**, 469; b) G. De Munno, M. Julve, G. Viau, F. Lloret, J. Faus, D. Viterbo, *Angew. Chem.* **1996**, *108*, 1931; *Angew. Chem. Int. Ed. Engl.* **1996**, *35*, 1807; c) R. Cortés, L. Lezama, J. L. Pizarro, M. I. Arriortua, T. Rojo, *Angew. Chem.* **1996**, *108*, 1934; *Angew. Chem. Int. Ed. Engl.* **1996**, *35*, 1810.

[9] a) S. Eggert, I. Affleck, M. Takahashi, *Phys. Rev. Lett.* **1994**, *73*, 332; b) R. B. Griffiths, *Phys. Rev.* **1964**, *133*, A768; c) see ref [10].

[10] C. N. Yang, C. P. Yang, *Phys. Rev.* **1966**, *150*, 327.

[11] J. Curely, F. Lloret, M. Julve, *Phys. Rev. B* **1998**, *58*, 11465.

[12] N. Metropolis, A. W. Rosenbluth, M. N. Rosenbluth, A. H. Teller, E. Teller, *J. Chem. Phys.* **1953**, *21*, 1087.

[13] K. Steiner, W. Willing, U. Müller, K. Dehnicke, *Z. Anorg. Allg. Chemie* **1987**, *555*, 7.

[14] F. A. Mautner, H. Krischner, Ch. Kratky, *Z. Kristallogr.* **1985**, *172*, 291.

[15] F. A. Mautner, H. Krischner, Ch. Kratky, *Monatsh. Chem.* **1988**, *119*, 509.

[16] M. A. S. Goher, T. C. W. Mak, *Inorg. Chim. Acta* **1985**, *223*, 99.

[17] M. E. Gross, T. Siegrist, *Inorg. Chem.* **1992**, *31*, 4898.

[18] M. Atam, U. Mueller, *J. Organomet. Chem.* **1974**, *435*, 71.

[19] M. W. Wemple, D. M. Adams, K. S. Hagen, K. Folting, D. N. Hendrickson, G. Christou, *J. Chem. Soc. Chem. Commun.* **1995**, 1591.

[20] M. A. Halcrow, J. S. Sun, J. C.Huffman, G. Christou, *Inorg. Chem.* **1995**, *34*, 4167.

[21] G. De Munno, T. Poerio, G. Viau, M. Julve, F. Lloret, *Angew. Chem.* **1997**, *109*, 1531; *Angew. Chem. Int. Ed. Engl.* **1997**, *36*, 1459, and references cited therein.

[22] a) A. Escuer, R. Vicente, F. A. Mautner, M. A. S. Goher, *Inorg. Chem.* **1997**, *36*, 1233; b) S. S. Tandon, L. K. Thompson, M. E. Manuel, J. N. Bridson, *Inorg. Chem.* **1994**, *33*, 5555; c) L. K. Thompson, S. S. Tandon, M. E. Manuel, *Inorg. Chem.* **1995**, *34*, 2356.

[23] E. Ruiz, J. Cano, S. Alvarez, P. Alemany, *J. Am. Chem. Soc.* **1998**, *120*, 11122.

[24] A. Escuer, C. J. Harding, Y. Dussart, J. Nelson, V. McKee, R. Vicente, *J. Chem. Soc. Dalton Trans.* **1999**, 223.

[25] K. Binder, D. W. Heermann, in *Monte Carlo Simulation in Statistical Physics. An introduction*, 3rd ed. (Ed. P. Fuld), Springer, Berlin, **1997**.

[26] J. Cano, Y. Journaux, *Mol. Cryst. Liq. Cryst.* **1999**, *335*, 1397.

[27] O. Kahn, *Molecular Magnetism*, VCH, New York, **1993**, chapter 6.

[28] R. Cortés, L. Lezama, J. L. Pizarro, M. I. Arrioruta, T. Rojo, *Inorg. Chem.* **1994**, *35*, 2697.

[29] N. Walker, D. Stuart, *Acta Crystallogr. Sect. A* **1983**, *39*, 158.

[30] G. M. Sheldrick, *SHELXS-86, Program for the Solution of Crystal Structure*, Universität Göttingen, Germany, **1986**.

[31] G. M. Sheldrick, *SHELX-76, A computer program for crystal structure determination*, University of Cambridge, England, **1976**.

[32] G. M. Sheldrick, *SHELXL-93, Program for the Refinement of Crystal Structure*, Universität Göttingen, Germany, **1993**.

[33] *SHELXTL 5.03 (PC-Version), Program library for the Solution and Molecular Graphics*, Siemens Analytical Instruments Division, Madison, WI (USA), **1995**.

[34] A. L. Spek, *PLUTON-92*, University of Utrecht, 3584, CH Utrecht (The Netherlands), **1992**.

Received: May 5, 1999 [F1769]

© WILEY-VCH Verlag GmbH, D-69451 Weinheim, 2000